ECS Transactions, 35 (1) 2035-2043 (2011)
10.1149/1.3570194 ©The Electrochemical Society

Impact of the Volatile Cr-species' Attack on the Conductivity of $La(Ni,Fe)O_3$

M.K. Stodolny[a,*,z], B.A. Boukamp[b,**], F.P.F. van Berkel[a]

[a]Energy research Centre of the Netherlands, Hydrogen and Clean Fossil Fuels, 1755 ZG, Petten, The Netherlands
[b]Dept. of Science and Technology & MESA+ Institute for Nanotechnology, University of Twente, 7500 AE, Enschede, The Netherlands

This study demonstrates the detrimental impact of Cr on the electronic conductivity of a $LaNi_{0.6}Fe_{0.4}O_3$ (LNF) porous cathode layer at 800 ºC. Vapor transport of Cr-species, originating from a porous metallic foam, and subsequent reaction with LNF results in a decrease of the electronic conductivity of the LNF-layer. Cr has been detected throughout the whole cross-section of the LNF-layer. Transmission electron microscopy revealed that Cr is gradually incorporated into the LNF-grains, while Ni is proportionally expelled. The progressing Cr deposition and penetration into the LNF-grains most likely explains the electronic conductivity drop. The Cr-poisoning impact on the electronic conductivity of the LNF porous layer is considerably smaller at 600 ºC than at 800 ºC. A tentative mechanism for the Cr attack and its influence on the electronic conductivity of the LNF layer will be presented.

Introduction

The perovskite $LaNi_{0.6}Fe_{0.4}O_3$ (LNF) is a candidate material for various intermediate temperature solid oxide fuel cell (IT-SOFC) applications where relatively cheap interconnect materials such as chromia forming ferritic stainless steels are used. High electronic conductivity and a thermal expansion coefficient matching that of zirconia (1), together with a claimed high Cr resistance (2-4), make LNF a promising candidate for use as cathode current collecting layer, interconnect protective coating and/or electrochemically active cathode layer in SOFC systems utilizing metallic interconnects.

For reliable operation of LNF in a Cr-containing environment, further investigation regarding the actual tolerance of LNF towards Cr should be undertaken, especially in the view of recent findings demonstrating the occurrence of a solid-state reactivity of LNF with chromia at 800 ºC (5,6). This study investigates to which extent the electronic conductivity of the LNF layer is affected by a non-contact exposure to Cr. Transport of Cr-species is known to take place by

* Electrochemical Society Student Member.
** Electrochemical Society Active Member.
z E-mail: stodolny@ecn.nl

solid-state diffusion and through vapor phase transport (7,8). The aim of this study is to describe and clarify the mechanism of the attack of volatile Cr-species and its impact on the electronic conductivity of a porous LNF-layer. The electronic conductivity is monitored under open circuit conditions and, in order to accelerate the poisoning impact, in a semi-stagnant Cr saturated atmosphere. The exposed porous LNF layer closely resembles porous SOFC cathode layers that have been investigated in other studies (9-11). Based on those studies a tentative mechanism for the Cr attack and its influence on the electronic conductivity of the LNF layer will be presented.

Experimental

LNF layers were prepared using $LaNi_{0.6}Fe_{0.4}O_3$ (Praxair, 99.9%) powder. The mechanical support used during the conductivity measurements was composed of a 3 mol% yttria doped zirconia (3YSZ) electrolyte sheet covered with 40 mol% gadolinia doped ceria (40GDC). The LNF paste was screen printed on top of the 40GDC layer and sintered at 1250 °C. Subsequently, gold contacts were attached at both ends of the LNF layer to allow the measurement of the sheet conductivity (9,12).

In order to measure the electronic conductivity, each sample was heated in a quartz tube flushed with 20% O_2 and 80% N_2 at a flow rate of 100 ml/min, to the operating temperature of 800 or 600 °C. After reaching the operating temperature, the impedance was measured using a Solartron 1255 frequency response analyzer in conjunction with a Solartron 1287A electrochemical interface in a semi-four-probe configuration. The specific electronic conductivity was calculated from the sheet resistance of the LNF layer and the LNF layer thickness.

The conductivity measurements were performed as function of time in a Cr-free (reference) and in a Cr-containing environment. For the Cr-poisoning experiments an ITM-14 metallic porous foam (Plansee AG, Reutte, Austria) was used as Cr source. The laser-cut foam was pre-oxidized for 100 h at 800 ºC prior to the experiment to assure a steady and reproducible Cr release rate (13). The ITM-14 foam sheet was positioned 1 mm above the 1×1 cm^2 area of the LNF layer without any direct contact.

After carrying out the conductivity measurements the samples were analyzed by field emission scanning electron microscopy, using a JEOL JSM 6330F FEG-SEM equipped with an EDX detector (ThermoNoran's Pioneer NORVAR). LNF-layers exposed to Cr were analyzed by means of inductively-coupled plasma-optical emission spectroscopy (ICP-OES), using a Varian Vista AX PRO CCD. The Cr-exposed sample chosen for the transmission electron microscopy (TEM) analyses was prepared by the method of Dimple Grinding/Polishing and argon ion beam etching. TEM analyses were performed using Philips CM300ST-FEG TEM equipped with a Gatan Tridiem energy filter and a Thermo Fisher NORAN System Six EDX analyzer with a Nanotrace EDX detector.

Results and Discussion

Conductivity evolution of LNF at 800 ºC

Figure 1 shows the electronic conductivity evolution with time of the LNF layers at 800 ºC in Cr-free and in Cr-containing atmospheres. The reference sample showed a relatively stable electronic conductivity for a testing period of 250 h. The LNF sample exposed to volatile Cr species exhibited a dramatic loss in electronic conductivity within the first 50 h, then a semi-linear conductivity decline could be observed in the time period of approximately 100-300 h, subsequently a second steep conductivity drop appeared after 320 hours of the exposure to volatile Cr species.

The influence of the different LNF layer microstructures, in terms of particle size and available grain surface area, on the rate of the electronic conductivity loss, caused by the volatile Cr species attack, will be discussed in detail in a follow-up paper (14).

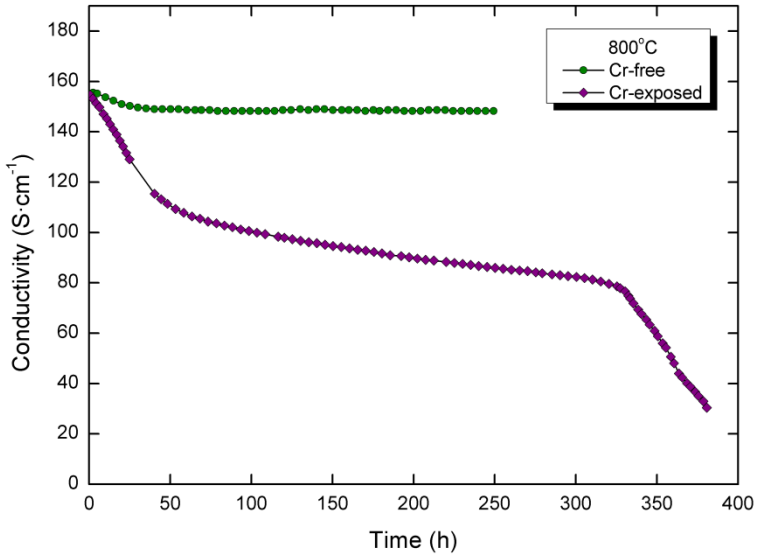

Figure 1. Electronic conductivity evolution at 800 ºC for the Cr-free and Cr-exposed LNF layer.

Cr distribution in a Cr-exposed LNF layer

This section deals with a change of the nominal LNF layer composition as a function of exposure time to volatile Cr-species and the resulting distribution of Cr throughout the layer.

Figure 2 shows the amount of Cr deposited in the LNF-layers exposed for different time periods at 800 ºC. The Cr-content, as obtained from the ICP-OES measurements on the powder scraped off the Cr-exposed LNF-layers, increased with the exposure time suggesting that the decline in the electronic conductivity, as shown in Figure 1, is related to the amount of Cr deposited in the layer. The Cr-content presented in Figure 2 is relative to the initial cationic composition of the LNF-layer.

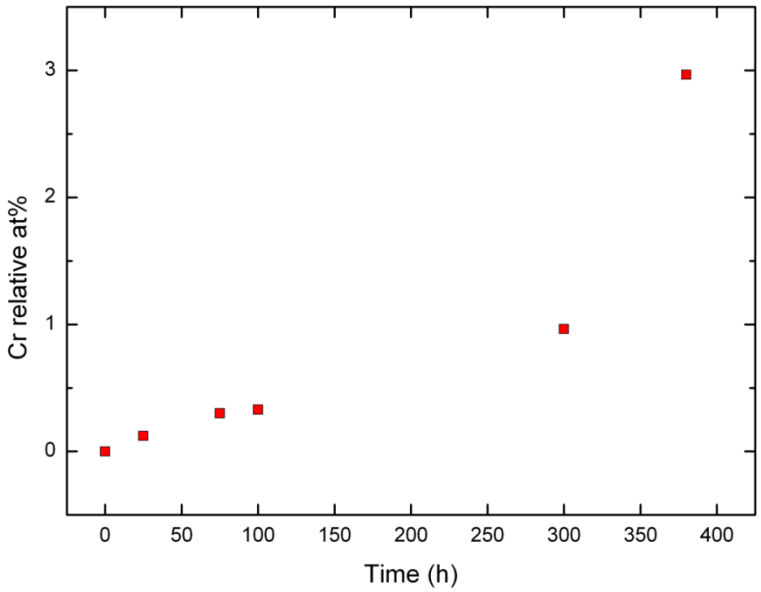

Figure 2. The amount of Cr deposited in the Cr-exposed LNF-layer as function of the exposure time.

The distribution of Cr in the LNF layer exposed to volatile Cr-species for 380 h at 800 ºC was provided by Energy Dispersive X-ray spectroscopy (EDX). Figure 3 shows the SEM-EDX elemental mapping on a polished cross-section of the Cr-exposed LNF layer. It demonstrates that Cr was spread throughout the entire cross-section of the layer without any significant areas of agglomeration, at least not visible with the available resolution (being circa 1μm^3) of the used SEM-EDX technique. Therefore, a technique offering higher detection resolution, below the 1μm scale, is required to investigate the exact Cr location. To this end, TEM-EDX (Transmission Electron Microscopy-EDX) was used, as discussed in the following section. The uniform distribution of Cr throughout the Cr-exposed LNF-layer, as observed by SEM-EDX, indicates that Cr entered the porous LNF-layer via a vapor phase transport and that Cr volatile species were attracted to the LNF grain surface. This attraction might be understood by comparing the enthalpies of formations and the relative thermodynamic stability of the perovskites: $LaCrO_3$ > $LaFeO_3$ > $LaNiO_3$ (15).

Cr distribution in a Cr-exposed LNF grain

From the sample examined with SEM-EDX (Figure 3) a section was taken which was used to prepare a TEM-specimen for analysis of the Cr distribution within a single grain. A preliminary TEM screening of different locations was performed in order to select a representative grain for in-depth analyses by Bright Field TEM imaging (BF-TEM), Energy Filtered TEM (EF-TEM), and TEM-EDX.

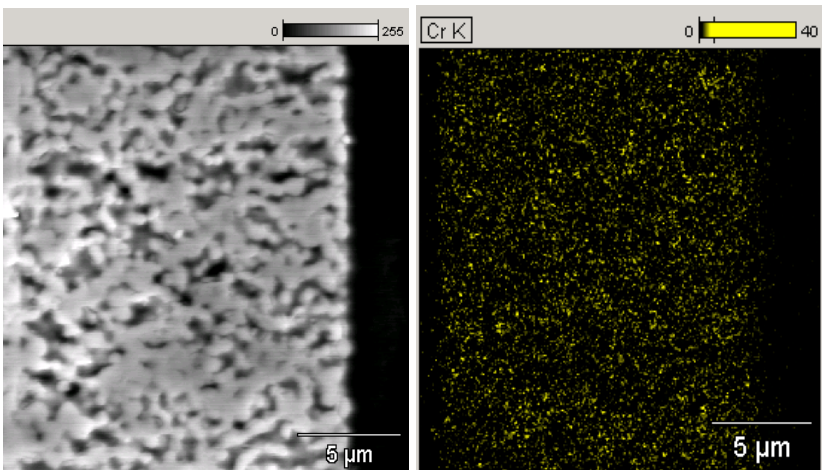

Figure 3. SEM-EDX elemental mapping of Cr throughout the Cr-exposed LNF layer (380 h at 800 ºC).

BF-TEM, EF-TEM, and TEM-EDX.

At first instance the Energy Filtered TEM analysis (EF-TEM using a 3-window method) was used to obtain the Cr distribution across the adjacent LNF grains depicted in a Bright Field TEM image (Figure 4a). The corresponding EF-TEM Cr map, presented in Figure 4b, shows a Cr enrichment close to the grains' edges. However, due to the possible edge artifacts in the EF-TEM analysis, further confirmation of the Cr enrichment was obtained by Energy Dispersive X-ray spectroscopy (EDX) in the region marked by an arrow in Figure 4b.

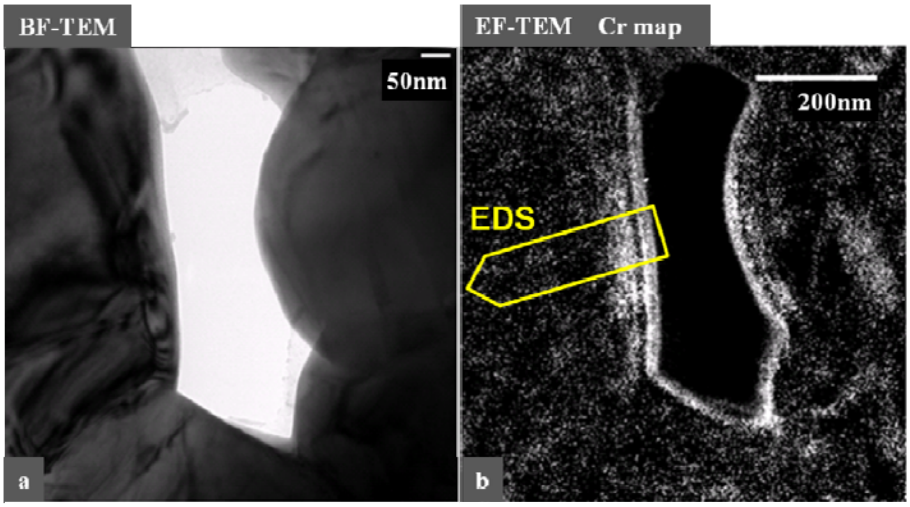

Figure 4. (a) BF-TEM image and corresponding (b) EF-TEM Cr map of the sliced Cr-exposed LNF-grains (380 h at 800 ºC).

TEM-Energy Dispersive X-ray spectroscopy (TEM-EDX) in a Point-and-Shoot way (i.e. by focusing the electron beam with a spot diameter of 3.5 nm) was performed on the thinned grain,

at a distance of 10, 40 and 300 nm from the grain's edge. The measurement was repeated 3 times in close vicinity of each spot to obtain a representative average. The locations of the TEM-EDX analyses are depicted on an inset of a Bright Field TEM image (BF-TEM) in Figure 5.

Figure 5 shows Ni, and Cr concentrations detected in different distances from the grain's edge. The concentrations of A and B constituents of the perovskite ABO_3 (i.e. La, Ni, Fe and Cr) were combined together to 100% and therefore Ni and Cr concentrations, shown in Figure 5, are referred to as relative at%. In the center of the grain (300 nm spot) no Cr was detected, while the amount of Ni resembled the nominal concentration of LNF. This finding proves that the center of the grain was unaffected by Cr. At a distance of 40 nm from the grain's edge Ni was considerably depleted and substituted by Cr. Close to the grain's edge (10 nm spot) a massive replacement of Ni by Cr was observed.

The observed gradients of elements suggest that Cr diffused into the particle, while Ni diffused out of the particle. The removed Ni formed NiO crystals in the voids of the LNF layer (16). These results imply that the rate of Cr-incorporation into the LNF-grain is very likely to be determined by the diffusion rates of Ni-ions moving outward and Cr-ions moving inward the grain in the B-sublattice of the ABO_3-perovskite network.

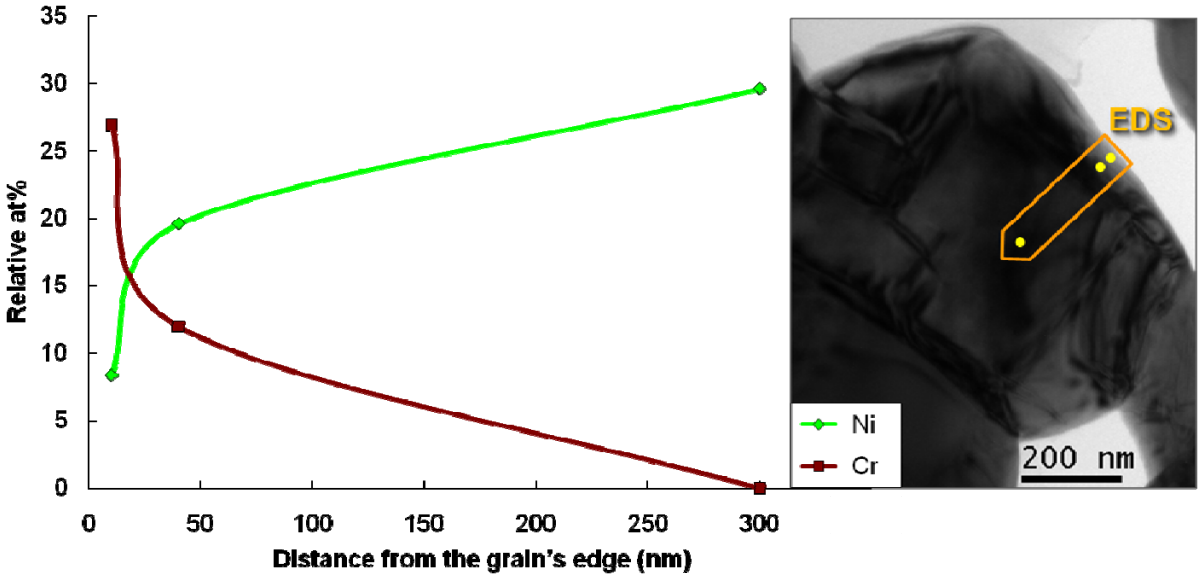

Figure 5. Ni and Cr concentration variations across the sliced Cr-exposed LNF-grain (TEM-EDX). The left figure shows the elemental distribution over the grain distance indicated by the arrow and TEM-EDX spots in the bright field TEM image in the right figure. The smoothed lines, connecting elemental concentration values, are only a guide to the eye.

The gradient of Cr concentration throughout the grain obtained by TEM-EDX (Figure 5) supports the results of the EF-TEM Cr map that showed a Cr enrichment close to the LNF-grains' edges (Figure 4b).

The influence of the incorporated Cr and removed Ni on the crystal structure of the Cr affected grains has been investigated using Selected Area Electron Diffraction (SAED). The obtained results will be reported in a follow-up paper (16).

Conductivity evolution at 600 ºC

To investigate the impact of the Cr-exposure at lower temperatures, where reactivity is supposed to be thermally hindered (5,6), a similar conductivity experiment was repeated at 600 ºC. Figure 6 shows the evolution of the electronic conductivity as a function of time for the LNF layer exposed to volatile Cr-species at 600 ºC. For comparison, Figure 6 contains also the results of the conductivity study at 800 ºC. Compared to the sample exposed at 800 ºC, the other sample exposed at 600 ºC exhibited considerably smaller electronic conductivity drop. Only ~ 10% electronic conductivity was lost after exposure at 600 ºC, in contrast to ~ 80% electronic conductivity loss at 800 ºC after the same time of operation of 380 h.

The observed deterioration of the electronic conductivity occurring both at 800 ºC and 600 ºC suggests that a comparable electronic conductivity degradation mechanism took place at both operating temperatures considered. However, the significant differences in the electronic conductivity drop indicate that the poisoning process took place at different rates. This could be due to the thermally induced differences in the amount of Cr species released by the Cr-source and/or in the rate of Cr diffusion into the LNF grain.

At 600 ºC the reactivity of LNF with gas phase Cr-species is still detectable (Fig. 6). However, taking into account that in the present study the Cr-poisoning conditions are intentionally chosen to be severe, in order to accelerate the poisoning impact, the stability of the LNF towards the Cr-poisoning should be regarded as rather high and relatively promising in a Cr saturated atmosphere at 600 ºC.

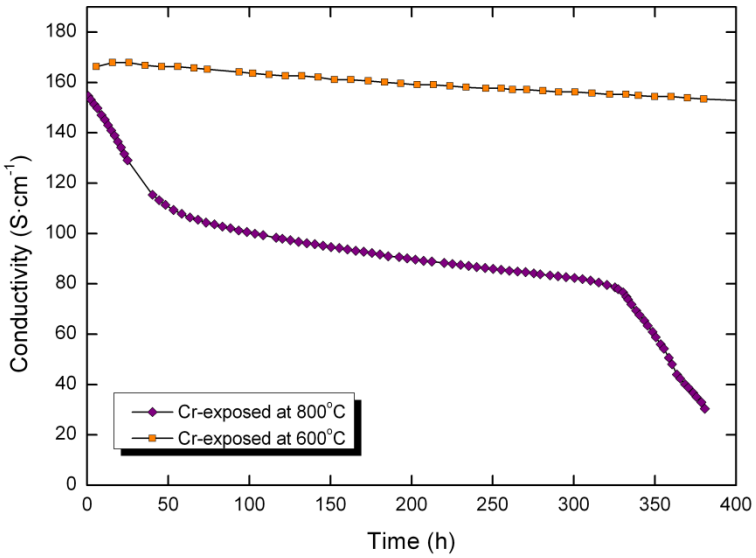

Figure 6. Electronic conductivity evolution in time of Cr-exposed LNF layers at 600 ºC and 800 ºC.

Conclusions

Mechanism of Cr attack and its influence on the electronic conductivity of the LNF

1. Vapor transport of Cr-species and subsequent reaction with LNF resulted in a decrease of the electronic conductivity of the LNF-layer.

2. The SEM-EDX investigation of the cross-section of the LNF-layer exposed to volatile Cr species at 800 ºC, indicated that Cr entered the porous LNF-layer via vapor phase transport and that the reaction takes quite homogeneously place over the entire surface.

3. The TEM-EDX analysis performed on the scale of an LNF particle revealed a considerable gradient in the perovskite composition throughout the LNF-grain. It appears that Cr is gradually incorporated into the grain, while Ni is proportionally expelled. The Cr-enrichment is in line with previous findings of solid state reactivity of LNF with chromia, also showing the replacement of Ni by Cr in the LNF perovskite (5,6).

4. The ICP-OES analysis of the Cr-exposed layers shows that the Cr-content increases with exposure time, suggesting that the decline in the electronic conductivity is related to the amount of Cr deposited in the porous LNF layer.

5. The decrease in the electronic conductivity of LNF during Cr-exposure at 600 ºC is taking place at a significantly lower rate than at 800 ºC. For the same time of operation of 380 h, only 10% electronic conductivity is lost after exposure at 600 ºC, in contrary to 80% electronic conductivity loss after exposure at 800 ºC.

6. A relatively small impact of the volatile Cr-species saturated atmosphere on the electronic conductivity of the LNF-layer at 600 ºC suggests that the use of $LaNi_{0.6}Fe_{0.4}O_3$ perovskite for various IT-SOFC purposes, where ferritic steels are being used as bipolar plates, still might be a viable option. However, further investigation in a real SOFC system needs to be undertaken to assess the feasibility of LNF as a Cr-tolerant material.

Acknowledgements

This work was partly supported by the European Commission, as part of the European Project SOFC600 (SES6-CT-2006-020089). The ECN KIMEX project is acknowledged for funding. Adrien Signolet is acknowledged for his involvement in this study during his traineeship at ECN. Jan Pieter Ouweltjes is thanked for helpful discussions and comments. ECN Engineering & Services (Materials Testing & Consultancy group) is thanked for the SEM-EDX and ICP-OES analysis. Enrico G. Keim (MESA+ institute NanoLab, University of Twente) is gratefully acknowledged for assistance with the TEM analyses.

References

(1) R. Chiba, F. Yoshimura, and Y. Sakurai, *Solid State Ionics*, **124**, 281 (1999).
(2) T. Komatsu, H. Arai, R. Chiba, K. Nozawa, M. Arakawa, and K. Sato, *Electrochem. Solid-State Lett.*, **9,** A9J (2006).
(3) Y.D. Zhen, A.I.Y. Tok, S.P. Jiang, F.Y.C. Boey, *J. Power Sources*, **170**, 61 (2007).
(4) G.Y. Laua, M. C. Tucker, C. P. Jacobson, S. J. Visco, S. H. Gleixner, and L. C. DeJonghe, *J. Power Sources*, **195**, 7540 (2010).
(5) M. Stodolny, F. P. F. van Berkel, and B. A. Boukamp, *ECS Transactions*, **25 (2)** 2915-2922 (2009).
(6) M. K. Stodolny, B. A. Boukamp, D. H. A. Blank, and F. P. F. van Berkel, *J. Electrochem. Soc.* **158** (2), B112-B116 (2011).
(7) M. C. Tucker, H. Kurokawa, C. P. Jacobson, L. C. De Jonghe, and S. J. Visco, *J. Power Sources*, **160**, 130 (2006).
(8) K. Hilpert, D. Das, M. Miller, D. H. Peck, and R. Weiss, *J. Electrochem. Soc*, **143**, 3642 (1996).
(9) F. P. F. van Berkel, M. Stodólny, M. Sillessen, and J. P. Ouweltjes, in *Proceedings of the 8th European Solid Oxide Fuel Cell Forum*, Vol. A0621, pp. 1–9, European Fuel Cell Forum (2008).
(10) M. K. Stodolny, F. P. F. van Berkel, and J. P. Ouweltjes, *ECN Internal Communication*, To be submitted.
(11) M. K. Stodolny, B. A. Boukamp, D. H. A. Blank, and F. P. F. van Berkel, To be submitted.
(12) J. P. Ouweltjes, M. van Tuel, M. Sillessen, and G. Rietveld, *Fuel Cells* **9, 873** (2009).
(13) M. Stanislowski, J. Froitzheim, L. Niewolak, W. J. Quadakkers, K. Hilpert, T. Markus, and L. Singheiser, *J. Power Sources*, **164**, 578-589 (2007).
(14) M. K. Stodolny, B. A. Boukamp, D. H. A. Blank, and F. P. F. van Berkel, To be submitted.
(15) J. Cheng, A. Navrotsky, X. Zhou, and H. Anderson, *J. Mater. Res.*, **20**, No.1, 191 (2005).
(16) M. K. Stodolny, B. A. Boukamp, D. H. A. Blank, and F. P. F. van Berkel, To be submitted.